



ADVECTION BOUNDARY LAW FOR SOUND TRANSMISSION ATTENUATION OF PLANE AND SPINNING GUIDED MODES

Emanuele De Bono^{1*}

Morvan Ouisse^{1*}

Jacky Mardjono⁵

Manuel Collet²

Martin Gillet^{1*}

Kevin Billon²

Edouard Salze³

Hervé Lissek⁴

Maxime Volery⁴

¹ SUPMICROTECH, Université de Franche-Comté, CNRS, Institut FEMTO-ST, F-25000 Besançon, France

²Univ. Lyon, Ecole Centrale de Lyon, LTDS UMR 5513, F-69134 Ecully, France

³Univ Lyon, Ecole Centrale de Lyon, LMFA UMR CNRS 5509, 69134 Ecully, France

⁴Ecole polytechnique Fedrale de Lausanne, Laboratoire de traitement des signaux LTS2,
Route Cantonale, 1015 Lausanne, Switzerland

⁵ Safran Aircraft Engines, F-75015, Paris, France

ABSTRACT

Sound attenuation along a waveguide is a highly demanded research field, for applications ranging from heating and air-conditioning ventilation systems, to aircraft turbofan engines. Electroacoustic devices and digital control have provided the tools for crafting innovative liners where the boundary condition can be programmed. The most straightforward idea is to program classical local impedance operators. Nevertheless, it might be worthy to navigate off the beaten track, and try to target boundary operators which could never be physically produced by purely passive treatments. In this contribution, we focus the attention on a particular boundary law, called advective, as it possesses a convective character achieved thanks to the introduction of the first spatial derivative. After introducing such special boundary condition, we implement it on an electroacoustic liner and demonstrate its potentialities in enhancing the transmission loss in acoustic waveguides with flow. We present results for both plane and spinning modes attenuation. Numerical simulations and experimental implementations demonstrate the potential-

ity of this boundary law, opening the doors toward boundary operators involving spatial derivatives for wave propagation control.

Keywords: noise control, spinning modes, spatial boundary operators, impedance control

1. INTRODUCTION

Reducing fuel pollution of airplanes has brought up another equally complex challenge for the aeronautic industry: the noise pollution. The new generation of Ultra-High-By-Pass-Ratio turbofan engines while considerably reducing fuel consumption, threatens higher noise levels at low frequencies because of its larger diameter, lower number of blades and rotational speed. This is accompanied by a shorter nacelle, leaving less available space for acoustic treatments. In this context, a progress in the liner technology is highly demanded, prospecting alternative solutions to classic liners. The Salute H2020 project has taken up this challenge, proposing electro-active acoustic liners, made up of loudspeakers (actuators) and microphones (sensors). The electro-active means allow to control the local impedance, but also to conceive alternative boundary laws, involving the spatial gradient of sound pressure. The advection boundary law [1–3], involving a first order spatial operator, has opened the doors toward innovative programmable boundary laws. The objective of this contribution is to present the potentialities

*Corresponding author: emanueledeb88@hotmail.it.

Copyright: ©2023 Emanuele De Bono et al. This is an open-access article distributed under the terms of the Creative Commons Attribution 3.0 Unported License, which permits unrestricted use, distribution, and reproduction in any medium, provided the original author and source are credited.



of such boundary condition for the transmission mitigation of both plane waves and spinning modes, in waveguides with significant air-flows.

2. PLANE WAVES ATTENUATION

The advection boundary law, as defined in [3], reads:

$$Z_{Loc}[\partial_t v_n(t)] = \partial_t p + U_b \partial_x p, \quad (1)$$

where the operator $Z_{Loc}[\bullet]$ is the local impedance operator applied to the normal boundary acceleration $\partial_t v_n(t)$. For classical locally reacting liners, this operator relates the local acceleration to the time derivative of the local sound pressure $\partial_t p$. Our advection law includes an additional term, given by U_b times the spatial gradient of pressure. U_b can be called advection speed. This boundary condition involves a first order spatial gradient, which hence implies nonlocality of the boundary reaction and non-reciprocity (as it is of first order). This operator has been implemented on a programmable boundary made up of electroacoustic resonators (ER), as described in [2,3,5] by piloting the electrical current $i(s)$ in the speaker coil. Its expression in the Laplace domain is given in Eq. (2):

$$i(s) = H_{loc}(s)\hat{p}(s) + H_{grad}(s)\hat{\partial}_x p(s), \quad (2)$$

where $\hat{p}(s)$ and $\hat{\partial}_x p(s)$ are the estimated local pressure and its x -derivative on each speaker diaphragm, in the Laplace variable s . Experimentally, on each EA, the local pressure is estimated by averaging the four microphones on the EA corners, while the x -derivative is estimated by a first-order finite difference. The transfer function $H_{loc}(s)$ is in charge of cancelling out the loudspeaker own dynamics (classically written in terms of Thiele-Small parameters [6]), and enforce the local target dynamics, whilst the transfer function $H_{grad}(s)$ enforces the spatial gradient dependence.

Such Electroacoustic Liner has been covered by a thin wiremesh in order to protect it from the airflow, and applied on the “Caiman” waveguide, showed in Figure 1. Here we are interested only in the plane wave regime.

Figure 2 shows the scattering performances when Mach is 0.15. In case of mean-flow, we must distinguish the downstream (plus sign, in green) from the upstream propagation (minus sign, in red). Observe that the advection control demonstrates higher capacities with respect to local impedance control, for both upstream and downstream propagation.

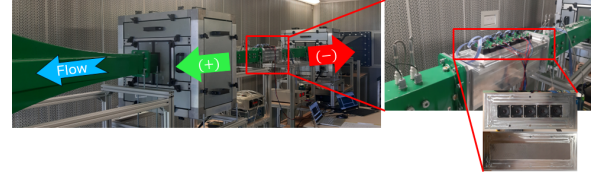


Figure 1. Left: “Caiman” wind tunnel, available in the Laboratory of Fluid Mechanics and Acoustics in the Ecole Centrale de Lyon. The downstream and upstream sense of propagation are indicated by the green and red arrows respectively. Right: zoom on the treated section with our electroacoustic liner covered by a wiremesh.

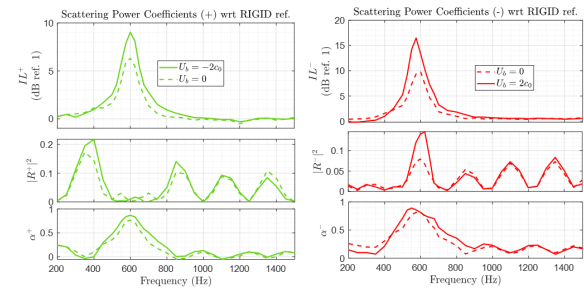


Figure 2. Scattering power coefficients for Mach 0.15 in the downstream (left) and upstream (right) senses. Advection operator ($U_b = -2c_0$, solid lines), or local impedance control ($U_b = 0$, dashed lines).

3. SPINNING MODES ATTENUATION

We wondered if such advection boundary control could be interesting for reducing noise radiation from a turbofan.

3.1 Simulations

In order to investigate the potentialities of generally impedance controlled liner for noise mitigation in a waveguide of large circular cross-section characterized by a multi-modal acoustic environment, some numerical simulations have been conducted in COMSOL Multiphysics. In particular, the performances of the boundary treatment in a waveguide are obtained by the multi-modal Scattering matrix, where the reflection or transmission coefficients of the Scattering matrix links two possibly different acoustic modes.



Figure 3. Illustration of the scattering problem in acoustic waveguide, with guided modes amplitudes definition on the left side and on the right side of the acoustically treated segment.

3.2 Multi-modal scattering

In this section we present the solution of the multi-modal scattering problem in case of absence of mean-flow ($M_x = 0$). This problem is defined as in Eq. (3), where the terms C_μ^+ , A_γ^- , A_ν^+ and C_σ^- are illustrated in Figure 3. The transmission coefficient matrix for example, $[T_{\mu,\nu}^+]$, links the amplitudes of the incident guided modes $\{A_\nu^+\}$ (with varying mode index “ ν ”) to the amplitudes of the transmitted guided modes $\{C_\mu^+\}$ (of varying index “ μ ”).

$$\begin{bmatrix} \{C_\mu^+\} \\ \{A_\gamma^-\} \end{bmatrix} = \begin{bmatrix} [T_{\mu,\nu}^+] & [R_{\mu,\sigma}^-] \\ [R_{\gamma,\nu}^+] & [T_{\gamma,\sigma}^-] \end{bmatrix} \begin{bmatrix} \{A_\nu^+\} \\ \{C_\sigma^-\} \end{bmatrix} \quad (3)$$

After having defined the multi-modal scattering problem, we present now some interesting results concerning the attenuation of multi-modal sound propagation achieved by both a purely local impedance B.C., and an *advected* boundary law. The advection law has been modified to oppose the spinning modes, by imposing the boundary advection along the azimuthal direction, see Eq. (4).

$$Z_{Loc}[\partial_t v_n(t, x, R, \theta)] = (\partial_t + U_b \partial_{arc\theta}) p(t, x, R, \theta). \quad (4)$$

We present here the simulation results obtained by such control law applied on a cylinder model with same sizes as the turbofan nacelle presented in the next section, but without flow. Figure 4 shows the comparison of the intensity scattering coefficients performances between purely local ($U_b = 0$) and advected ($U_b = -2c_0$) boundary control, plotted in solid and dotted lines respectively. Observe that the boundary advection significantly reduces the transmission of energy (mostly by enhancing the backward reflection) for spinning exciting modes (with first index different from 0), without altering the performances relative to the non-spinning ones (with first index equal to 0).

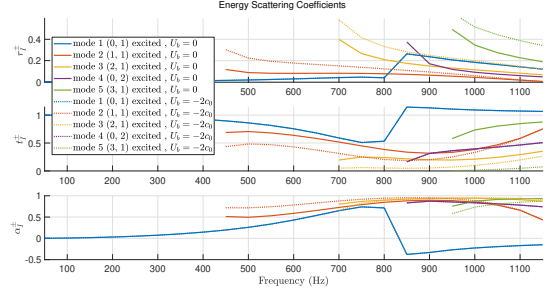


Figure 4. Comparison of intensity scattering coefficients in case of $U_b = 0$ (solid lines) and $U_b = -2c_0$ (dotted lines).

These computations have very much helped to gain confidence about the expectable results in the experimental campaign.

3.3 Experimental test-bench

The test-bench is a reproduction (scale 1 to 3) of a turbofan engine [4], called “Phare 2”, available in the Laboratory of Fluid Mechanics and Acoustics in the Ecole Centrale de Lyon. The intake boundaries of the nacelle were treated by a circular electroacoustic liner, see Figure 5. The radiated sound field was recovered by a movable antenna of microphones placed all around the intake, see Figure 6. The gray ball in the picture is a turbulence screen to reduce the turbulence level sucked into the engine. Moreover, two rings of microphones are placed upstream and downstream the liner, as illustrated in the schematics of Figure 7, in order to retrieve the azimuthal modal content of the sound field before and after the electroacoustic liner.

In this case, the sound field is much more complex. But, due to the rotational speed of the turbofan, the predominant modes propagating in the nacelle are typically of spinning type. Figure 8 shows the insertion loss (IL) relative to one antenna’s microphone, with respect to a control-off reference level. In Figure 9 and 10, you see the average level of azimuthal modes around the target frequency, respectively upstream and downstream with respect to the liner. Observe that here we are interested in reducing the radiation upstream the liner. The IL plot of Figure 8 demonstrates how a counter-rotating azimuthal advection ($U_b = -2c_0$) is capable to reduce the noise radiation around the Blade-Passing-Frequency (BPF) with respect to a purely local impedance control ($U_b = 0$).

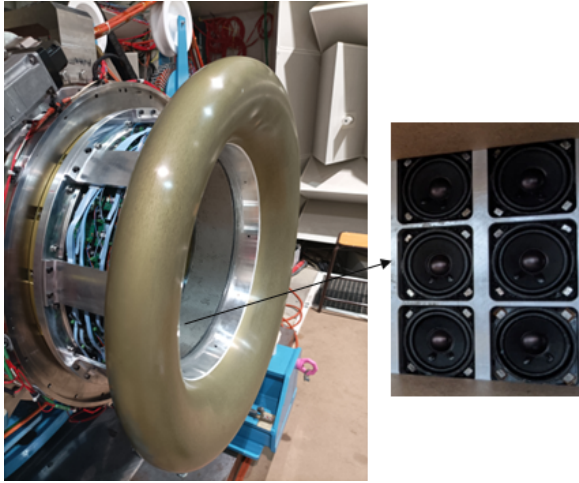


Figure 5. Electroacoustic liner at the intake of the nacelle of “Phare 2”.

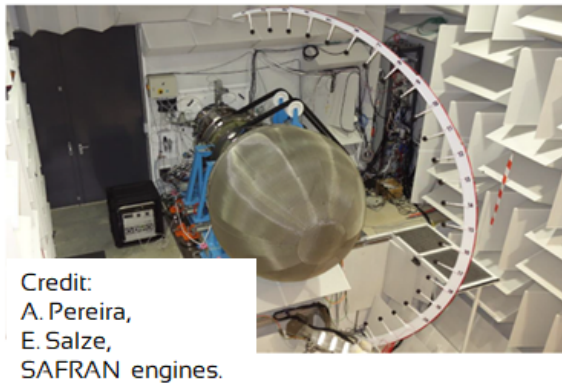


Figure 6. Photo of the “Phare 2” facility.

This is due to an enhanced attenuation of the principal azimuthal mode at the upstream section, as shown in Figure 9.

4. CONCLUSIONS

We have presented various results obtained by a boundary condition operator, called Advection Law, which is an interesting example of nonlocal control of sound waves. Such B.C. has been first tested against plane wave propagation, and then adapted to turbofan noise, when spinning modes are predominant. We demonstrated its potentiality in overcoming the limitations of purely local impedance

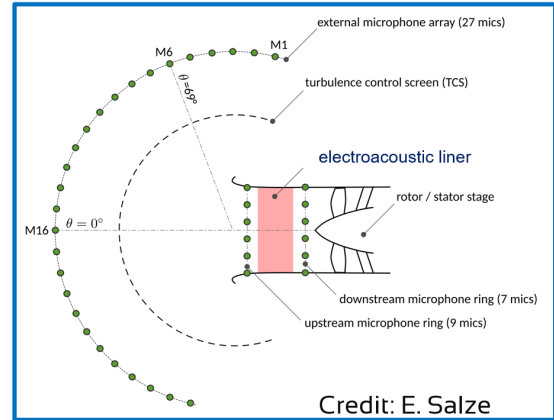


Figure 7. Sketch of the “Phare 2” facility.

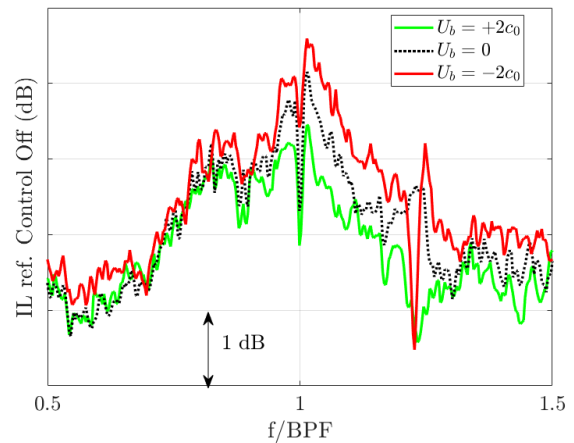


Figure 8. Results in terms of IL on a microphone of the antenna, in case of $U_b = 2c_0$ (green line), $U_b = 0$ (dotted black line) and $U_b = -2c_0$ (red line).

control laws, opening the doors toward programmable boundaries involving spatial gradients of sound pressure.

5. ACKNOWLEDGMENTS

The SALUTE project has received funding from the Clean Sky 2 Joint Undertaking under the European Union’s Horizon 2020 research and innovation programme under grant agreement N 821093. This publication reflects only the author’s view and the JU is not responsible for any use that may be made of the information it contains.

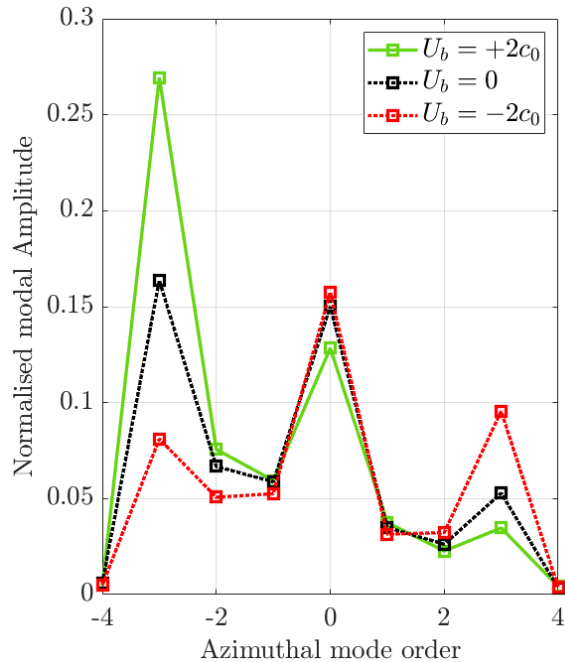


Figure 9. Results in terms of upstream modal contents, in case of $U_b = 2c_0$ (green line), $U_b = 0$ (dotted black line) and $U_b = -2c_0$ (dotted red line).

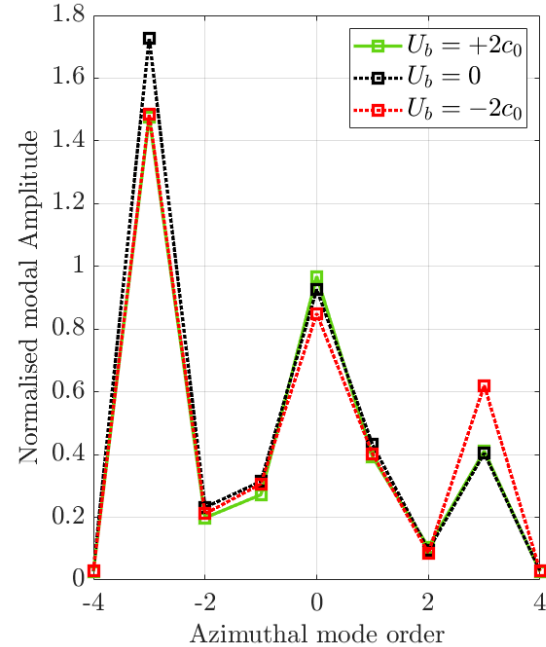


Figure 10. Results in terms of downstream modal contents, in case of $U_b = 2c_0$ (green line), $U_b = 0$ (dotted black line) and $U_b = -2c_0$ (dotted red line).

6. REFERENCES

- [1] M. Collet, P. David, and M. Berthillier, "Active acoustical impedance using distributed electro-dynamical transducers," *The Journal of the Acoustical Society of America*, vol. 125, no. 2, pp. 882–894, 2009.
- [2] S. Karkar, E. De Bono, M. Collet, G. Matten, M. Ouisse, and E. Rivet, "Broadband Nonreciprocal Acoustic Propagation Using Programmable Boundary Conditions: From Analytical Modeling to Experimental Implementation," *Physical Review Applied*, vol. 12, p. 054033, nov 2019.
- [3] E. De Bono, *Electro-active boundary control for noise mitigation: local and advective strategies*. PhD thesis, Université de Lyon, 2021.
- [4] A. Pereira, E. Salze, J. Regnard, F. Gea-Aguilera, and M. Gruber, "New modular fan rig for advanced aeroacoustic tests-Modal decomposition on a 20" UHBR fan stage," in *25th AIAA/CEAS Aeroacoustics Conference*, p. 2604, 2019.
- [5] K. Billon, E. De Bono, M. Perez, E. Salze, G. Matten, M. Gillet, M. Ouisse, M. Volery, H. Lissek, J. Mardjono, and Others, "Experimental assessment of an active (acoustic) liner prototype in an acoustic flow duct facility," in *Health Monitoring of Structural and Biological Systems XV*, vol. 11593, p. 115932L, International Society for Optics and Photonics, 2021.
- [6] L. L. Beranek and T. Mellow, *Acoustics: Sound Fields and Transducers*. Oxford OX5 1GB, UK: Academic Press, 2012.